DOI: 10.1002/ejic.200600438

Chiral Recognition of Mesoporous SBA-15 with an Incorporated Chiral Porphyrin

Huan-Bao Fa,[a,d] Lang Zhao,[b] Xing-Qiao Wang,*[a] Ji-Hong Yu,[b] Yi-Bing Huang,[c] Min Yang,[a] and De-Jun Wang[a]

Keywords: Chiral recognition / Porphyrins / Mesoporous materials / SBA-15

The incorporation of a chiral porphyrin into the mesoporous molecular sieves SBA-15 by reactions of the surface OH group with an amino group of the porphyrin and its chiral recognition were studied. The resultant material was analyzed by a combination of techniques and it was confirmed that the channels of SBA-15 have been filled with chiral porphyrins, leaving the mesopores unaffected. The investigation of chiral recognition of the porphyrin and the composite SBA-15 shows that the incorporated SBA-15 has a clear CD spectral signal of the chiral porphyrin and exhibits different chiral recognition abilities for small amino acids. The D-alanine is more tightly bound to the mesoporous composite SBA-15 than its optical antipode.

Introduction

Chiral recognition is an attractive subject in the area of host-guest chemistry, since it is a fundamental process for a range of chemical and biological phenomena.[1–3] Several types of host molecules for chiral recognition studies have been reported[4–10] because of their biological and chemical importance. Among them, porphyrins are relatively accessible molecules and have been used in recognition studies for the past two decades.[11–16] However, the use of porphyrins for chiral recognition has been restricted due to their poor stability in solution. A useful means to improve the stability of porphyrins is by encapsulating them into microporous materials such as zeolites, since molecular encapsulating is an emerging technology with potential applications in separation, chemical sensing, and catalysis.[17] However, for natural faujasite and synthetic zeolites X and Y the supercage diameter and the aperture to the cages are only 0.7–1.3 nm, which is too small for big complexes such as porphyrin substrates and products to diffuse in and out.[18] The discovery of the mesoporous material SBA-15[19,20] by Zhao and coworkers in 1998 provided the materials needed to achieve porphyrin incorporation since the SBA-15 has a regular hexagonal array of uniform channels with diameters 4.6–30 nm, high internal surface area of about 700–1000 $m^2 g^{-1}$, and high thermal and hydrothermal stabilities.

Incorporation of metal complexes into mesoporous SBA-15 for catalytic purposes has been extensively investigated.[21–26] However, studies on the incorporation of chiral metal complexes into SBA-15 and their chiral recognitions are limited[27] and there are no reports on incorporation of chiral porphyrins and their chiral recognitions. It is, therefore, important to study this system and to focus on chiral recognition of the host for small chiral molecules. It has been proposed that the enantioselectivity of the host for amino acids could be effectively enhanced by constructing a specific chiral environment derived from protected amino acids on the host porphyrin. In this research, we designed and synthesized a porphyrin that contains an amino acid on the porphyrin plane (Figure 1) and incorporated the porphyrin molecule with chiral recognition into the channels of SBA-15 to give it chiral recognition functions. Methods reported to date for organic complex fixation include: (a) impregnation,[28,29] (b) attachment to amine ligands provided by the modification of a mesoporous material surface with an organosilane,[29–31] (c) encapsulation during hydrothermal synthesis,[32] (d) ion exchange between the organic complex cation and the template surfactant species in the non-calcined mesoporous material,[32] and (e) covalent bonding of the amine-functionalized porphyrin to sites created in mesoporous material by doping with Nb.[33] It is well known that the interior surface of SBA-15 is covered with OH groups, so reduction of the nitro group on the porphyrin circumference led to the formation of aminogen with amino groups linking to OH groups of the SBA-15 through hydrogen bonding. In this paper, we report the results of our studies on the incorporation of a chiral porphy-

[a] College of Chemistry, Jilin University,
2519 Jiefang Road, Changchun 130021, China
[b] Key Laboratory of Inorganic Synthesis & Preparative Chemistry, Jilin University,
Changchun 130023, China
[c] Key Laboratory of Molecular Enzymology and Engineering,
Changchun 130021, China
[d] College of Chemistry and Chemical Engineering, Chongqing University,
Chongqing 400044, China

rin into SBA-15, and chiral recognition of the mesoporous composite SBA-15/porphyrin using a combination of techniques such as X-ray diffraction (XRD), transmission electron microscopy (TEM), UV/Vis spectroscopy, nitrogen adsorption, and circular dichroism (CD) spectroscopy. At the same time, the enantioselectivity of the chiral porphyrin for an amino acid ester in solution was studied for comparison with the SBA-15/porphyrin.

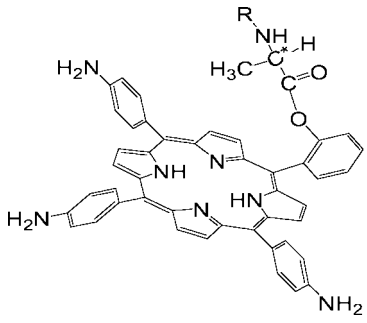

Figure 1. Chemical structure of the chiral porphyrin (R = Boc).

Results and Discussion

General Features of the Synthesized Material

The X-ray powder diffraction (XRD) patterns of SBA-15 before (Figure 2, b) and after (Figure 2, a) the incorporation of the chiral porphyrin are given in Figure 2. The XRD patterns of pure SBA-15 and SBA-15/porphyrin show strong (100) peaks, suggesting that framework stability of the mesoporous material is well maintained when the chiral porphyrin is incorporated into the channels of SBA-15. It is to be noted that the relative intensities of (110) and (200) scattering reflections were dramatically decreased for the composite consisting of both the porphyrin and SBA-15 when compared to the same bands for pure SBA-15. The change is interpreted as indicating that the porphyrins are dispersed in the mesoporous channels. TEM measurements were used to analyze the structure of the SBA-15. From the TEM image (Figure 3), it is seen that large ordering domains with highly ordered hexagonal (Figure 3, b) and

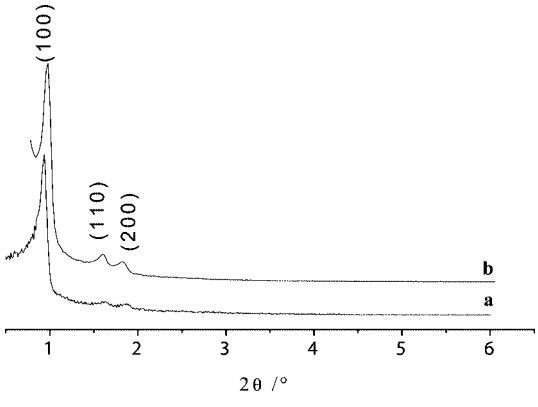

Figure 2. XRD patterns of SBA-15 samples with (a) and without (b) the incorporated chiral porphyrin.

strutlike arrays (Figure 3, a) exist. The SBA-15 after incorporation of chiral porphyrin is shown in Figure 4. When comparing this to Figure 3, it is clear that the hexagonal structure of SBA-15 is preserved after the chiral porphyrin incorporation. However, the TEM images of Figure 4 (part b [110], and part a [100]) show that the hexagonal channels of SBA-15/porphyrin become shaggier. The observed difference can probably be attributed to incorporation of the chiral porphyrin into the channels of SBA-15.

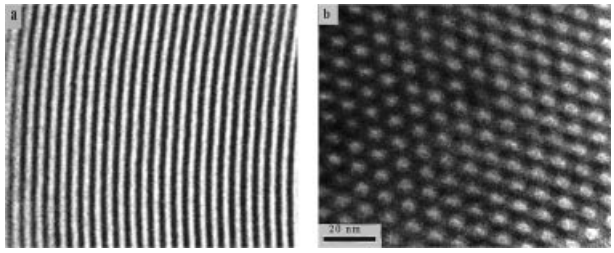

Figure 3. TEM images of SBA-15 along the (a) [100] and (b) [110] directions.

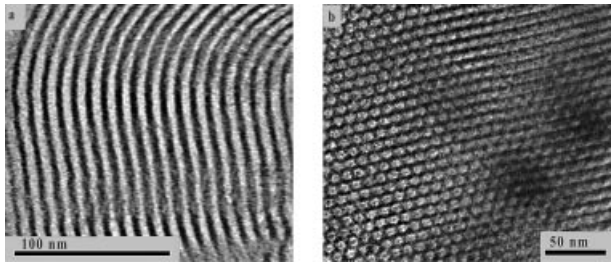

Figure 4. TEM images of SBA-15 with incorporated chiral porphyrin along the (a) [100] and (b) [110] directions.

UV/Vis diffuse reflectance spectrum of the chiral porphyrin, SBA-15/porphyrin, and pure SBA-15 are given in Figure 5. The pure SBA-15 has no characteristic absorption bands over the entire spectral region (Figure 5, a). The chiral porphyrin itself has the Soret bands (438 nm) and four Q-bands (526, 573, 662, 729 nm) (Figure 5, c). The SBA-15/porphyrin has absorption bands at 425 (Soret band), 518, 560, and 698 nm (Figure 5, b). Compared with the pure complex, the Soret band of the chiral porphyrin in SBA-15 is shifted toward shorter wavelengths. This can be attributed to interactions of the porphyrin with the interior surface hydroxyl groups of SBA-15. It has been shown that oxide supports have strong perturbations on the absorption maxima and molar absorption coefficients.[34] A comparison of the characteristic absorption bands of the chiral porphyrin incorporated SBA-15 with that of the chiral porphyrin confirms the incorporation of the chiral porphyrin into the SBA-15 channels. When the chiral porphyrin was incorporated, interactions of the ligands of the porphyrin with their local chemical environment changed the symmetry of the porphyrin. Because of these interactions, the polarity of the surroundings of the porphyrin is increased, as evidenced by the shifts of the absorption bands toward higher energy (shorter wavelength) in the UV/Vis spectra given above.

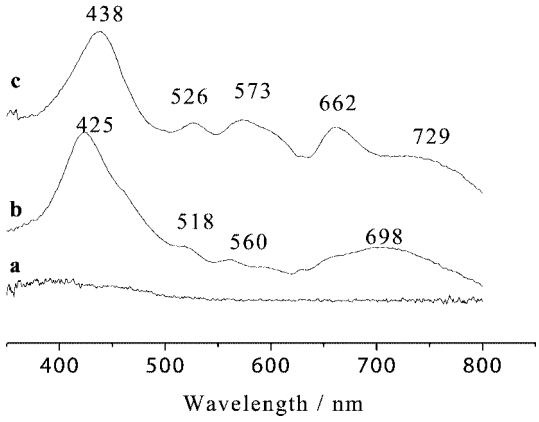

Figure 5. UV/Vis absorption spectra of SBA-15 before (a) and after (b) the incorporation of chiral porphyrin, and also the chiral porphyrin on its own (c).

In order to understand better the texture of the mesoporous composite SBA-15/porphyrin, the nitrogen isothermal adsorption technique was employed. Nitrogen adsorption/desorption isotherms for SBA-15 and SBA-15/porphyrin are shown in Figure 6. When porphyrins were incorporated into SBA-15, the sharpness of the inflection was significantly reduced at the P/P_0 range from 0.45 to 0.9, and the inflections were shifted slightly toward lower P/P_0 ranges. The inflection point of the relative pressure is related to a diameter in the mesopore range, and the sharpness of these steps indicates the uniformity of the mesopore size distribution.[35,36] Compared to pure SBA-15, the mesoporous composite SBA-15/porphyrin showed a reduction of sharpness, indicating less uniformity of the mesopore size distribution. Table 1 summarizes the results of N_2 adsorption analyses. After incorporation of chiral porphyrin into SBA-15, the S_{BET}, V_t, and D_{BJH} values for SBA-15/porphyrin were 427 $m^2 g^{-1}$, 0.66 $cm^3 g^{-1}$, and 9.0 nm, respectively, and 540 $m^2 g^{-1}$, 0.88 $cm^3 g^{-1}$, and 9.8 nm for pure SBA-15, respectively. Therefore, all parameters of SBA-15/porphyrin decreased compared with pure SBA-15. This is fully consistent with the results of the XRD, UV/Vis, and TEM studies and confirms that the porphyrin was successfully incorporated into the interior surface of the channels of SBA-15. There is a slight decrease of the average pore size (D_{BJH}) from 9.8 to 9.0 nm (Figure 6, B), which indicates that some of the nanometer-shaggier void space of the host silica is open, although a portion of the channels may be blocked by the porphyrin molecules. The space is important for guest molecules to diffuse into the host silica, and to contact chiral porphyrin molecules for reactions to proceed.

Table 1. Physical and surface properties of selected samples.

Sample	S_{BET}[a] [$m^2 g^{-1}$]	V_t [$cm^3 g^{-1}$]	D_{BJH} [nm]
SBA-15	540	0.88	9.8
SBA-15/porphyrin	427	0.66	9.0

[a] S_{BET}, BET specific surface area; V_t, total pore volume; D_{BJH}, pore diameter calculated using the BJH method.

The CD spectra of the chiral porphyrin in solution and the SBA-15/porphyrin in the solid phase are given in Figure 7. The SBA-15 incorporating chiral porphyrin gives CD signals while the pure SBA-15 does not have CD signals. This also confirms the results that the porphyrin has been

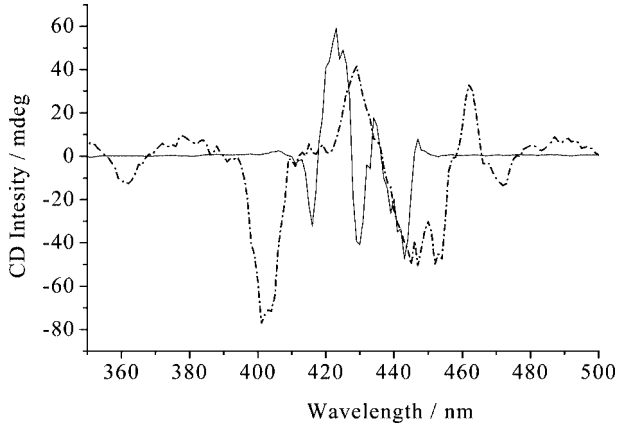

Figure 7. Circular dichroism spectra of the chiral porphyrin (solid line) (1×10^{-6} M) in chloroform and the SBA-15/porphyrin (dash dot line) (solid state) at 298 K.

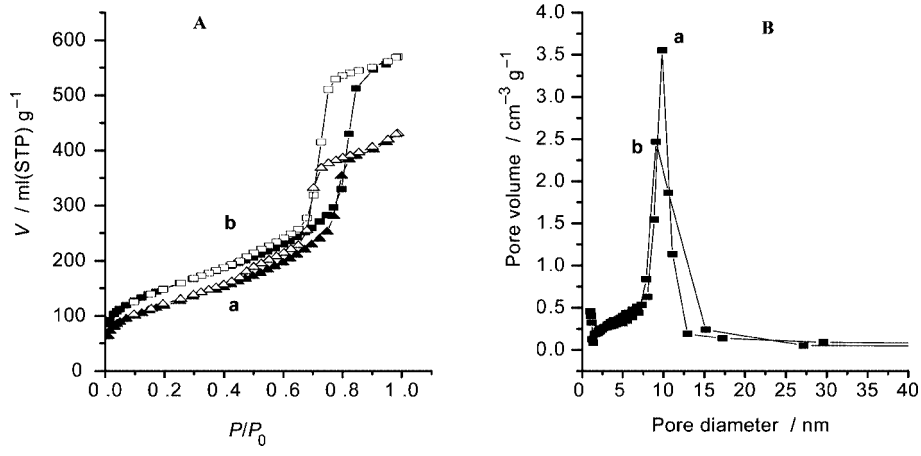

Figure 6. A: Nitrogen adsorption isotherms of pure SBA-15 (a) and SBA-15/porphyrin (b). B: Pore size distribution of the samples calculated from the adsorption branch of the isotherms using the BJH algorithm.

successfully incorporated into the channels of SBA-15. The great change in peak shape of the chiral porphyrin upon incorporation also demonstrates that incorporation has indeed occurred. Difference in peak shape is likely attributable to the influence of the channel of mesoporous material by interactions of porphyrins with OH groups of the SBA-15.

Chiral Recognition

To investigate comparatively the chiral recognition of the chiral porphyrin and mesoporous composite SBA-15/porphyrin for chiral amino acids, visible spectroscopy and circular dichroism spectra were employed to study the enantioselectivity of L and D amino acids.

Figure 8 shows circular dichroism spectra of porphyrin 1 before and after linking L-BocAla. The porphyrin 1 has no spectral signal, but porphyrin 3 has a strong CD spectral signal with a split Cotton effect around its Soret band when chiral amino acid is linked with porphyrin 1 by covalent bonding. The interaction between the excited states of chromophores in unsymmetrical environments gives circular dichroism curves with split Cotton effects.[37] There is strong exciton-coupled action between the porphyrin ring and the acylamide group. Porphyrin 3 exhibits complex curves around its Soret band (Figure 8, b). According to the Tinoco law,[38] the coupling between the electric and magnetic transition moments of the acylamide group and the electric transition moments of porphyrin chromophores leads to the observed Cotton effects.[13,39]

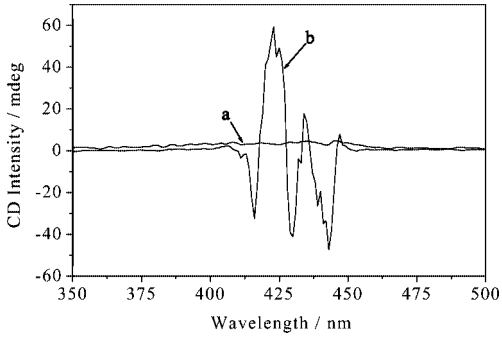

Figure 8. Circular dichroism spectra of porphyrin 1 (a) and chiral porphyrin 3 (b) (1×10^{-6} M).

Absorption spectra of chiral porphyrins binding with amino acid esters of varying concentrations are shown in Figure 9 and Figure 10, which suggest a stepwise binding of the chiral porphyrin with D- and L-alanine methyl ester ($AlaOCH_3$), respectively. The absorption spectral change in the Soret region shows an increase in intensity of the absorption band at 465 nm with a decrease of the absorption at 425 nm, displaying an isosbestic point at 440 nm, which indicates 1:1 complexation between the host and guest molecules. The association constant K is given by Equation (1).

$$\frac{1}{A_0 - A} = \frac{1}{K \cdot a} \cdot \frac{1}{C_L} + \frac{1}{a} \quad (1)$$

where A_0 is the absorbance of the porphyrin 3 solution at 425 nm, A is the absorbance in the presence of a guest at concentration C_L, and a is a constant. The quantity $1/(A_0 - A)$ has a linear relation to $1/C_L$; the association constant, K, can be obtained from the ratio of the intercept to the slope. The results of the association constant of D- and L-$AlaOCH_3$, are K_D = 9526 and K_L = 3834, respectively, which are much larger than that of ZnTPP.[40,41] This is because the electronic effect is more significant than the steric repulsion between the side chain of the amino acid ester and the branch group of the porphyrin. The association constant of D-$AlaOCH_3$ is larger than that of its optical antipode. The structure of the D-enantiomer of the guest molecules can be better aligned with the chiral porphyrin. The steric repulsion between the larger groups in the porphyrin and the L-enantiomer is unfavorable for "close binding" of the host and guest. Accordingly, the association of the porphyrin with the L-guest becomes weaker and the association constant smaller than that with the D-guest.

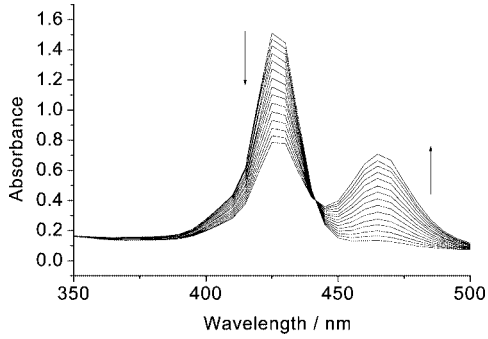

Figure 9. UV/Vis titration of the chiral porphyrin with L-$AlaOCH_3$ in chloroform at 298 K: [3] = 2×10^{-6} M; [L-$AlaOCH_3$] = 0, 0.1, 0.2, 0.3, 0.4, 0.5, 0.6, 0.7, 0.8, 0.9, 1.0, 1.1, 1.2, 1.3, and 1.4×10^{-4} M.

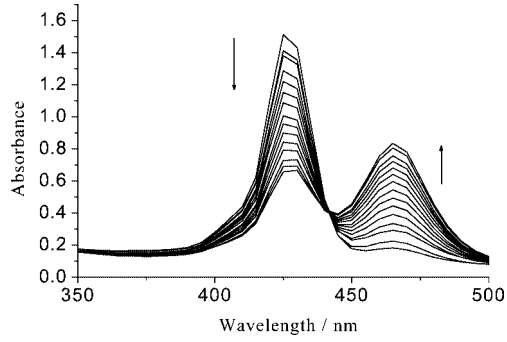

Figure 10. UV/Vis titration of chiral porphyrin with D-$AlaOCH_3$ in chloroform at 298 K: [3] = 1×10^{-6} M; [D-$AlaOCH_3$] = 0, 0.1, 0.2, 0.3, 0.4, 0.5, 0.6, 0.7, 0.8, 0.9, 1.0, 1.1, 1.2, 1.3, and 1.4×10^{-4} M.

The chiral porphyrin has a higher enantioselectivity in organic solutions, however, the tedious preparation, high cost, and weak stability of the porphyrin, and also the weak solubility of some amino acids in organic solutions obstruct the application of porphyrins in chiral recognition for amino acids. A good approach to circumvent this problem

is to incorporate porphyrins into SBA-15, facilitating the host-guest separation. To investigate the enantioselectivity of the mesoporous material SBA-15/porphyrin for chiral amino acids, a 10^{-3} M solution of L-alanine and D-alanine in distilled water was prepared. This solution (10 mL) of L-alanine and D-alanine was mixed with SBA-15 (5.6 mg) after incorporation of chiral porphyrin 3. While the mixture was stirred in a round-bottomed flask at room temperature, the solution was monitored by the CD technique. The changes in the CD spectra with time are shown in Figure 11 and Figure 12. Figure 11 gives the CD spectra of L-alanine with a positive response. As time passes, the response intensity of the solution of L-alanine decreases. The intensity at 30 min is half the intensity at 0 min. This indicates that L-alanine is absorbed into the channel and onto the surface of the mesoporous material.

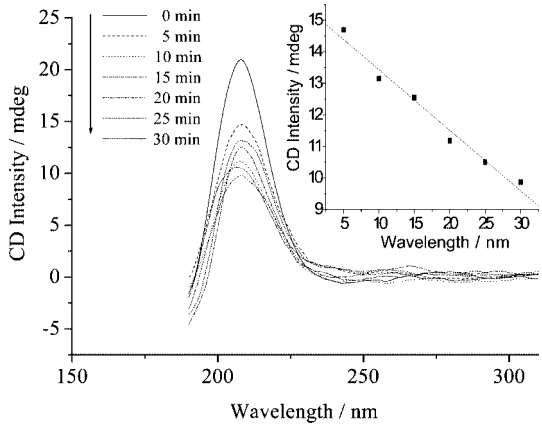

Figure 11. CD spectra of L-alanine at different times after being stirred with SBA-15/porphyrin. Inset shows the CD decrease (ΔCD) vs. time (min).

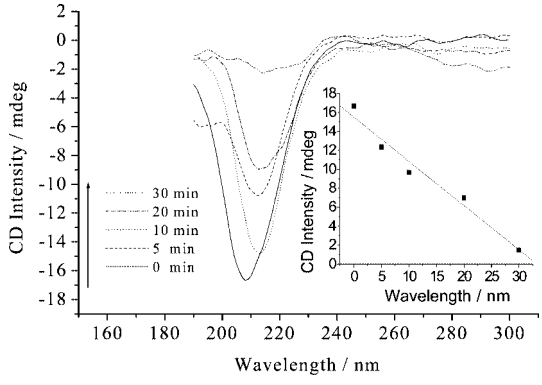

Figure 12. CD spectra of D-alanine solution at different times after being stirred with SBA-15/porphyrin. Inset shows the CD decrease (ΔCD) vs. time (min).

Comparing this with Figure 12, the CD spectra of D-alanine exhibit a negative response and a mirror image of L-alanine. The signal intensity of D-alanine also decreases with time. However, the difference is obvious compared with L-alanine in that the intensity at 30 min is very weak, nearly one ninth of that at 0 min (Figure 12). Also for the same 30 min, the changes of concentration of alanines in their liquid phase are evidently different (inset of Figure 11 and Figure 12). The linear regression parameter for L-alanine is 0.19, and –0.47 for D-alanine. All these results indicated that D-alanine couples more strongly with the mesoporous material, which is consistent with the results of the porphyrin with the amino acid ester. When the porphyrin was not incorporated into the SBA-15, the changes in the CD spectra of the alanines were the same. The observed difference is attributed to incorporation of the chiral porphyrin. The branch groups of the chiral porphyrin provide a chiral cavity for the guest molecules (small amino acids).

Conclusions

A combination of techniques such as XRD, TEM, UV/Vis, nitrogen adsorption, and CD spectroscopy was employed to confirm that we have successfully incorporated chiral porphyrins into the interior surface of the channels of mesoporous molecular sieves SBA-15. The SBA-15 has a clear CD spectra signal after the incorporation and shows different chiral recognition abilities for small amino acids such as L- and D-alanine. The above experiments demonstrate that the D-alanine is more tightly bound to the host than its optical antipode, which is consistent with the results of porphyrins in organic solutions. The investigation provides an available model for the application of chiral recognition.

Experimental Section

Materials and Physical Measurements: All reagents and solvents were of commercial reagent grade and used without further purification. Boc-alanine(BocAla) was purchased from Aldrich. The SBA-15 was synthesized according to ref.[19]

The powder diffraction of the solid materials was examined by using a Rigaku D/MAX X-ray powder diffractometer with a Cu-K_α X-ray source (λ = 0.154 18 nm). Transmission electron microscopic (TEM) images were performed with a JEOL JEM2011 electron microscope operating at 200 kV. UV/Vis spectra of solutions were collected with a Perkin–Elmer Lambda 2 spectrometer. Diffuse reflectance UV/Vis spectra of solids were recorded with a Perkin–Elmer Lambda 9 spectrometer. Circular dichroism (CD) spectra were performed with a JASCO-715 spectropolarimeter equipped with a thermostat cell compartment. Nitrogen adsorption measurements at 77 K were performed with a NOVA 2000e volumetric adsorption analyzer, samples were outgassed for 6 h in the degas port of the adsorption apparatus.

Synthesis of the Chiral Porphyrin: The synthesis procedure for the chiral porphyrin is illustrated in Scheme 1.The synthesis was based on the following procedures: The unsymmetrically phenyl-substituted porphyrin **1** was synthesized according to an adaptation of the general Rothemund method for synthesis of *meso*-tetraphenylporphyrins.[42] *o*-Hydroxybenzaldehyde (4.9 g, 1 equiv.) and *p*-nitrobenzaldehyde (6.1 g, 3 equiv.) were added to refluxing propionic acid (300 mL). Once the aldehydes had completely dissolved, freshly distilled pyrrole (6 mL, 4 equiv.) was added within 20 min and refluxed for 1 h. The reaction mixture was then cooled and allowed to stand overnight. After diluting with distilled water (500 mL) and adjusting the pH to 6–7 with aqueous sodium hy-

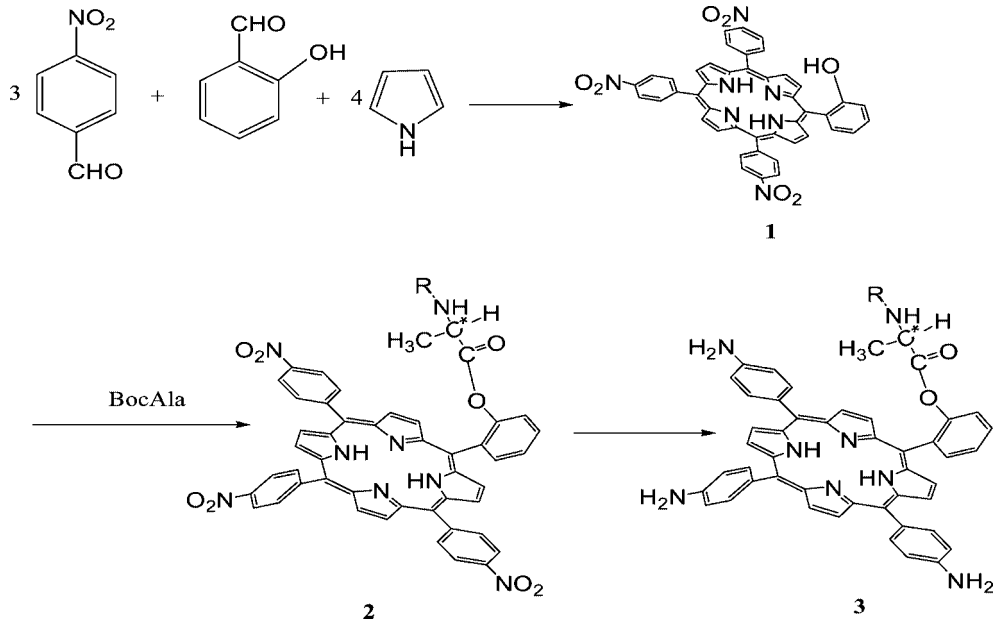

Scheme 1. Synthesis of the tailed chiral amino acid porphyrin chloroform at 298 K.

droxide (6 mol L^{-1}), filtration and hot water washing was performed five times. The obtained powder mixture, which was black-purple in color, was then dried in a vacuum oven at 80 °C overnight. The dried powder was extracted with chloroform until the extracts became colorless. After distilling off the solvents under a reduced pressure with a rotary evaporator, a black-purple crude product was obtained. The crude product was separated using silica gel column chromatography eluted first with dichloromethane followed by elution with a chloroform solution. The second elution was collected and the solvents evaporated to dryness, and the product was chromatographed a second time by column chromatography and then TLC. Porphyrin **1** was obtained at the end and dried in a vacuum oven at 80 °C overnight.

$C_{44}H_{27}N_7O_7$ (765.20): calcd. C 69.02, H 3.55, N 12.80; found C 68.85, H 3.50, N 12.63. Visible spectrum ($CHCl_3$): λ = 650, 590, 550, 515, 425 nm. IR (KBr): $\tilde{\nu}$ = 3442 (–OH), 3317 (pyrrole N–H) 2921 (C–H), 2850, (–CH_2–), 1515, 1346 (–NO_2) cm^{-1}. MALDI-TOF-MS: *m*/*z* = 765.5 $[M + 1]^+$.

BocAla (30 mg) was dissolved in thionyl chloride (50 mL). This solution was stirred at reflux for 12 h. Thionyl chloride was then removed by distillation under reduced pressure. The crude product was redissolved in benzene (60 mL) and triethylamine (5 mL). A solution of porphyrin 1 (50 mg) in benzene (10 mL) was added. The reaction was stirred for 10 h at reflux. The mixture separated into benzene and water. The organic layer was evaporated under reduced pressure. Flash column chromatography (silica gel, dichloromethane/ethanol, 3:1) afforded 14.1 mg (23%) of pure porphyrin 2.

$C_{52}H_{40}N_8O_{10}$ (936.29): calcd. C 66.66, H 4.30, N 11.96; found C 66.57, H 4.23, N 12.01. Visible spectrum ($CHCl_3$): λ = 650, 590, 550, 515, 425 nm. IR (KBr): $\tilde{\nu}$ = 3375 (CON–H), 3317 (pyrrole N–H), 2923 (–CH_3), 2852 (–CH_2–), 1699 (C=O) cm^{-1}. MALDI-TOF-MS: *m*/*z* = 937.2 $[M + 1]^+$.

Porphyrin **2** (24 mg) was dissolved in concentrated hydrochloric acid (36%, 20 mL) at room temperature, in a beaker, followed by addition of excess $SnCl_2{\cdot}2H_2O$ (100 mg). The resulting green mixture was quickly heated to 65–70 °C for 25 min, then cautiously neutralized with concentrated aqueous ammonia. Chloroform (20 mL) was added to the hot suspension and the mixture was stirred for 1 h. The chloroform layer was separated, the aqueous layer extracted several times with chloroform, and all chloroform extracts were combined and filtered. The chloroform solution was reduced in volume (10 mL) on a rotary evaporator, washed first with dilute aqueous ammonia then twice with water, dried with anhydrous sodium sulfate, and evaporated under reduced pressure. Flash column chromatography (silica gel, chloroform, the second elution) afforded 21.7 mg (89%) of pure porphyrin 3.

$C_{52}H_{46}N_8O_4$ (846.36): calcd. C 73.74, H 5.47, N 13.23; found C 73.58, H 5.39, N 13.34. Visible spectrum ($CHCl_3$): λ = 650, 590, 550, 515, 425 nm. IR (KBr): $\tilde{\nu}$ = 3429 (N–H), 3359 (CON–H), 3216 (pyrrole N–H), 2921 (–CH_3), 2850 (–CH_2–), 1700 (C=O) cm^{-1}. MALDI-TOF-MS: *m*/*z* = 847.4 $[M + 1]^+$.

Incorporation of Chiral Porphyrin into SBA-15: SBA-15 (100 mg) was mixed with porphyrin **3** (10 mg) in a round-bottomed flask (20 mL), and then chloroform (10 mL) was added and stirred for 48 h at room temperature. The solid was filtered and washed with chloroform until no absorption of porphyrin in the UV/Vis spectrum was seen from the solution. The solid was dried at room temperature. The original white powders of SBA-15 turned jade-green after adding the chiral porphyrin, which indicated inclusion of the porphyrins into the SBA-15 frameworks.

For quantitative determination of the porphyrin incorporated into the SBA-15, a mesoporous composite SBA-15/porphyrin sample (14 mg) was dissolved in aqueous sodium hydroxide solution (8 M) to destroy the framework. Thus the porphyrin in the mesoporous composite was released. The porphyrin was extracted with chloroform (10 mL), and the solution was diluted to 1/5 its concentration with chloroform. The OD value of the porphyrin at 425 nm is 0.3141. A reference solution was made with chiral porphyrin (0.5 mg) dissolved in chloroform (100 mL) and its OD value at 425 nm was measured to be 0.5022. By comparing this with the reference, the amount of porphyrin encapsulated in SBA-15 was determined to be 11.2 mg g^{-1} using Beer's law. Because there is no C element in pure SBA-15, the C elemental analysis of the mesopo-

rous composite was employed to obtain 0.83%. The amount of porphyrin was estimated to be 11.4 mg g^{-1}, which agrees with that obtained by Beer's law.

Acknowledgments

We gratefully acknowledge the support of this research by the National Science Foundation of China (20071014, 20473033).

[1] V. Schurig, F. Betschinger, *Chem. Rev.* **1992**, *92*, 873–888.
[2] W. H. Pirkle, T. Pochapsky, *Chem. Rev.* **1989**, *89*, 347–362.
[3] J. A. Gladysz, B. T. Boone, *Angew. Chem. Int. Ed. Engl.* **1997**, *36*, 550–583.
[4] M. Almaraz, C. Raposo, M. Martin, M. C. Calallero, J. R. Moran, *J. Am. Chem. Soc.* **1998**, *120*, 3516–3517.
[5] M. Rekarsky, Y. Inoue, *J. Am. Chem. Soc.* **2000**, *122*, 4418–4435.
[6] Z. Tao, T. S. M. Wan, K. Kwang, C. Che, *Anal. Chem.* **2000**, *72*, 5383–5393.
[7] K. Yannakopoulou, D. Mentzafos, I. M. Marridis, K. Dandika, *Angew. Chem. Int. Ed. Engl.* **1996**, *35*, 2480–2482.
[8] C. D. Stevenson, D. K. Cashion, *J. Org. Chem.* **2000**, *65*, 7588–7594.
[9] W. A. Tao, D. Zhang, E. Nikolaev, R. G. Cooks, *J. Am. Chem. Soc.* **2000**, *122*, 10598–10609.
[10] B. Chankvetadze, C. Yamamoto, Y. Okamoto, *Chem. Lett.* **2000**, *10*, 1176–1177.
[11] T. Mizutani, T. Ema, T. Tomita, Y. Kuroda, H. Ogoshi, *J. Am. Chem. Soc.* **1994**, *116*, 4240–4250.
[12] Y. Kuroda, Y. Kato, T. Higashioji, J. Hasegawa, S. Kawanawi, M. Takahashi, N. Shiraishi, K. Tanabe, H. Ogoshi, *J. Am. Chem. Soc.* **1995**, *117*, 10950–10958.
[13] H. Ogoshi, T. Mizutani, *Acc. Chem. Res.* **1998**, *31*, 81–89.
[14] R. J. Abraham, P. Leighton, J. K. M. Sanders, *J. Am. Chem. Soc.* **1985**, *107*, 3472–3478.
[15] R. P. Bonar-Law, L. G. Mackay, C. J. Walter, V. Marvaud, J. K. M. Sanders, *Pure Appl. Chem.* **1994**, *66*, 803–810.
[16] J. P. Collman, Z. Wang, C. Linde, L. Fu, L. Dang, J. I. Brauman, *Chem. Commun.* **1999**, 1783–1784.
[17] a) L. Andersson, *J. Chromatogr. B* **2000**, *745*, 3–13; b) K. Mosbach, *Anal. Chim. Acta* **2001**, *435*, 3–8; c) K. Haupt, K. Mosbach, *Chem. Rev.* **2000**, *100*, 2495–2504; d) B. Sellergen, *J. Chromatogr. A* **2001**, *906*, 227–252; e) D. Kriz, O. Ramstrom, K. Mosbach, *Anal. Chem.* **1994**, *66*, 2636–2639; f) B. Sellergen, *Angew. Chem. Int. Ed.* **2000**, *39*, 1031–1037; g) H. Shi, W.-B. Tsai, M. D. Garrison, S. Ferrari, B. D. Ratner, *Nature* **1999**, *398*, 593–597; h) S. Dai, *Chem. Eur. J.* **2001**, *7*, 763–768; i) M. A. Markowitz, P. R. Kust, G. Deng, P. E. Schoen, J. S. Dordick, D. S. Clark, B. P. Gaber, *Langmuir* **2000**, *16*, 1759–1765.
[18] H. Norman, *J. Coord. Chem.* **1988**, *19*, 25–38.
[19] D. Zhao, J. Feng, Q. Huo, N. Melosh, G. H. Fredrickson, B. F. Chmelka, G. D. Stucky, *Science* **1998**, *279*, 548–552.
[20] D. Zhao, Q. Huo, J. Feng, B. F. Chmelka, G. D. Stucky, *J. Am. Chem. Soc.* **1998**, *120*, 6024–6036.
[21] D. E. D. Vos, M. Dams, B. F. Sels, P. A. Jacobs, *Chem. Rev.* **2002**, *102*, 3615–3640.
[22] P. M. Rao, A. Wolfson, S. Kababya, S. Vega, M. V. Landau, *J. Catal.* **2005**, *232*, 210–225.
[23] Y. Cao, J. Hu, P. Yang, W. Dai, K. Fan, *Chem. Commun.* **2003**, 908–909.
[24] Ch. Nozaki, C. G. Lugmair, A. T. Bell, T. D. Tilley, *J. Am. Chem. Soc.* **2002**, *124*, 13194–13203.
[25] M. S. Zhu, S. H. Zhou, M. Hibino, I. Honma, *J. Mater. Chem.* **2003**, *13*, 1115–1118.
[26] M. Alvaro, A. Corma, D. Das, V. Fornés, H. García, *Chem. Commun.* **2004**, 956–957.
[27] D. Coutinho, A. O. Acevedo, G. R. Dieckmann, K. Balkus Jr, *J. Micropor Mesopor Mat.* **2002**, *54*, 249–255.
[28] H. M. Sung-Suh, Z. Luan, L. Kevan, *J. Phys. Chem. B* **1997**, *101*, 10455–10463.
[29] V. Schünemann, A. X. Trautwein, I. M. C. M. Rietjens, M. G. Boersma, C. Veeger, D. Mandon, R. Weiss, K. Bahl, C. Colapietro, M. Piech, R. N. Austin, *Inorg. Chem.* **1999**, *38*, 4901–4905.
[30] C.-J. Liu, S.-G. Li, W.-Q. Pang, C.-M. Che, *Chem. Commun.* **1997**, 65–66.
[31] C.-J. Liu, W.-Y. Yu, S.-G. Li, C.-M. Che, *J. Org. Chem.* **1998**, *63*, 7364–7369.
[32] B. T. Holland, C. Walkup, A. Stein, *J. Phys. Chem. B* **1998**, *102*, 4301–4309.
[33] L. Zhang, T. Sun, J. Y. Ying, *Chem. Commun.* **1999**, 1103–1104.
[34] a) P. A. Leermkers, H. T. Thomas, L. D. Weis, F. C. James, *J. Am. Chem. Soc.* **1966**, *88*, 5075–5083; b) G. Scheibe, F. Feichtmayr, *J. Phys. Chem.* **1962**, *66*, 2449–2455.
[35] B. L. Newalkar, J. Olanrewaju, S. Komarneni, *Chem. Mater.* **2001**, *13*, 552–557.
[36] Z. Luan, E. M. Maes, M. A. W. Van der Heide, D. Zhao, R. S. Czernuszewicz, L. Keven, *Chem. Mater.* **1999**, *11*, 3680–3686.
[37] a) N. Haraha, K. Nakanishi, *Circular Dichroic Spectroscopy-Exciton Coupling, in: Organic Stereochemistry*; University Science Books: Mill Valley, CA, **1983**; b) K. Nakanishi and N. Berova, in: *Circular Dichroism-Principles and Applications* (Eds.: K. Nakanishi, N. Berova, R. W. Woody), VCH Publishers, New York, **1994**, p. 361.
[38] I. Tinoco, *Adv. Chem. Phys.* **1962**, *4*, 113–117.
[39] T. Mizutani, T. Ema, T. Yoshida, Y. Kuroda, H. Ogoshi, *Inorg. Chem.* **1993**, *32*, 2072–2077.
[40] K. Anzai, T. Hosokawa, K. Hatano, *Chem. Pharm. Bull.* **1986**, *34*, 1865–1870.
[41] Y. Li, W. J. Ruan, C. Z. Wang, Z. A. Zhu, R. Chen, F. M. Miao, X. Wen, *Acta Scientiarum Naturalium Universtatis Nankaiensis* **1999**, *32*, 123–129.
[42] L. R. Milgrom, *J. Chem. Soc., Perkin Trans. 1* **1984**, 1483–1487.

Received: May 11, 2006
Published Online: September 7, 2006

